Pergamon

Int. J. Heat Mass Transfer. Vol. 41, No. 1, pp. 139–146, 1998

Printed in Great Britain
0017-9310/98 $19.00+0.00

PII: S0017-9310(97)00089-6

Effect of lateral and extended fins on heat transfer in a circulating fluidized bed

B. V. REDDY† and P. K. NAG‡

Department of Mechanical Engineering, Indian Institute of Technology, Kharagpur 721 302, India

(*Received* 11 *December* 1995 *and in final form* 4 *March* 1997)

Abstract—Experimental investigations are made in a hot circulating fluidized bed unit to study the effect of lateral, and lateral and extended fins together on heat transfer coefficient and on the rate of heat transfer. The circulating fluidized bed (CFB) unit consists of a riser column of 102 × 102 mm in bed cross-section (square), 5.25 m in height with the return leg of the same dimensions. Both liquid petroleum gas and coal are used as the fuel. A mathematical model is also proposed to predict the heat transfer coefficient to a water-wall test section with lateral and extended fins. The model results are compared with the present experimental data and also with those of published literature and a fair agreement has been observed. © 1997 Elsevier Science Ltd.

INTRODUCTION

To maintain the combustion temperature at an optimum level in a circulating fluidized bed (CFB) furnace, it is required for the walls of a CFB furnace to absorb a certain fraction of the heat input to the furnace. It is known that the heat input is proportional to the bed cross-section, whereas the heat absorption is proportional to the perimeter of the furnace. Large CFB boilers having high heat inputs are thus required to have either additional heating surfaces across the furnace or external heat exchangers. However, both the options are costly and may enhance the risk of tube surface erosion. Therefore, tubes with short fins could be employed to increase the surface area for more heat absorption. Basu *et al.* [1] made an experimental investigation to study the effect of fins on heat absorption in a cold CFB, under different operating conditions. Nag and Ali [2] reported heat transfer results for pin-fins in a cold CFB.

For the membrane water-wall tubes experimental results have been reported by Wu *et al.* [3, 4], Andersson and Leckner [5], and Golriz [6]. The provision of short extended fins in addition to lateral fins may be more effective in absorbing heat from the bed, but it may result in some change in bed hydrodynamics. For this combination, Basu and Ngo [7], and Reddy and Nag [8] reported some data. In the present work, experiments are conducted in a CFB unit to study the effect of lateral, and lateral and extended fins together with some relevant operating parameters on heat transfer. A mathematical model to predict heat transfer to the water-wall tube with lateral and extended fins is also proposed.

† Present address: Engineering College, Vellore 632 014, India.

‡ Author to whom correspondence should be addressed.

DETAILS OF EXPERIMENTAL UNIT

The investigations are conducted in a CFB unit which comprises of a main riser column of 102 × 102 mm in bed cross-section (square) with 250 mm thick brick walls, 5.25 m in height, with a return leg of the same dimensions (Fig. 1). It is made up of one layer of refractory bricks on the inside and one layer of insulating fire bricks on the outside. The gas–solid separation is achieved by means of an impact separator, in conjunction with a cyclone in series, both made up of mild steel. Air is supplied by a high-pressure centrifugal blower and the volume flow rate is measured with the help of an orifice meter (BS 1042) fixed in the air flow line before the distributor plate. The primary air is preheated by a 2 kW electric heater before it enters the distributor plate. The liquid petroleum gas is supplied to a burner located at a height of 0.75 m above the distributor plate. Static pressures are measured at 0.5 m intervals along the riser height with water tube manometers. Liquid petroleum gas and coal are burned in the unit.

The heat transfer test section is located at a height of 3.1 m above the distributor plate in the riser column. The test section with lateral fins is shown in Fig. 2(a). The water-wall probe with both lateral and extended fins is indicated in Fig. 2(b). First, the experiments are conducted with only lateral fins, and then with both lateral and extended fins together. Water is circulated through the test section, and the mass flow rate of water and the rise in water temperature are measured. Chromel–alumel thermocouples are used to measure the bed and probe surface temperatures. Local sand with a mean particle size (d_p) 248 μm and with a particle density (ρ_s) of 2350 kg m^{-3} is used as the bed material. The slide gate in the return leg is adjusted in such a way that a constant opening area of 10 cm^2 is maintained for the solids flow. The heat

NOMENCLATURE

A_f fin cross-sectional area, [m^2]
A_{f1}, A_{f2} cross-sectional areas of lateral and extended fins, [m^2]
A_{tot} total surface area of the test section with lateral and extended fins together [m^2]
A_{sf1} surface area of lateral fin [m^2]
A_{sf2} surface area of extended fin [m^2]
A_b bare tube surface area [m^2]
A_{uf} unfinned surface area of the tube [m^2]
b_1 lateral fin length [m]
b_2 extended fin length [m]
b_{2c} corrected extended fin length [m]
c_{pw} specific heat of water [kJ kg^{-1} K^{-1}]
d_p average diameter of bed solids [μm]
e_c, e_p, e_w, e_d emissivities of cluster, particle, probe wall and dispersed phase, respectively
f_{wb} wall-to-bed view factor
f_{wc} wall-to-cluster view factor
f_{wd} wall-to-dispersed phase view factor
$h_{(x)}$, h_{rad} convective and radiative heat transfer coefficients [W m^{-2} K^{-1}]
h, h_{avg} average heat transfer coefficient [W m^{-2} K^{-1}]
h_{fc} cluster radiative heat transfer coefficient [W m^{-2} K^{-1}]
h_d dispersed phase radiative heat transfer coefficient [W m^{-2} K^{-1}]
h_{eq} equivalent heat transfer coeffient based on total surface area including fins [W m^{-2} K^{-1}]
k_f thermal conductivity of fin material [W (m K)$^{-1}$]
m_w mass flow rate of water [kg s^{-1}]
OD outer diameter of the tube [m]
P perimeter of the fin [m]
q_c, q_r convective, radiative heat fluxes [W m^{-2}]
Q_{f1}, Q_{f2} heat flow rate to the lateral fin, extended fin [W]
Q_{uf}, Q_{tot} heat flow rate to the unfinned surface, and total heat flow rate to the test section [W]
Q_{t1} heat flow rate to the probe with lateral fins [W]
Q_{t2} heat flow rate t the probe with both lateral and extended fins together [W]
T temperature of the fin at any location [K]
T_B bed temperature [K]
T_S, T_w wall or probe mean surface temperature [K]
T_{wo}, T_{wi} water outlet and inlet temperature [K]
Y Volume fraction of solids in the dispersed phase.

Greek symbols
σ Stefan–Boltzman constant, 5.67×10^{-8} W m^{-2} K^{-4}
ε cross-sectional bed average voidage
ε_w voidage at the wall
ε_c cluster voidage
ξ non-dimensional fin length, x/b
θ dimensionless temperature of the fin, T/T_w
θ_b dimensionless temperature of the bed, T_B/T_w
ρ_{sus} cross-sectional average bed suspension density [kg m^{-3}]
ρ_S, ρ_P sand particle density [kg m^{-3}]
δ fraction of the wall area covered by clusters.

transfer coefficient is estimated by making energy balance at steady-state conditions.

The local cross-sectional average voidage of the bed (ε), and the cross-sectional average suspension density (ρ_{sus}) at the test section location are calculated from the measured pressure drop across the test section in the water-tube manometer.

$$\rho_{sus} = \rho_S(1-\varepsilon)+\rho_g\varepsilon.$$

Water-wall probe with lateral fins

The heat transfer coefficient is estimated by making energy balance at steady-state conditions. The middle tube with lateral fins on either side is considered for calculations. By taking into consideration the later fin efficiency

$$Q_{t1} = m_w cp_w(T_{wo}-T_{wi})$$
$$= h_{avg}(A_b+2A_{sf1}\times\eta_{f1})(T_B-T_S)$$

where A_b is the bare tube surface area exposed to the bed, A_{sf1} is the lateral fin surface area, η_{f1} is the lateral fin efficiency and T_B and T_S are the bed and probe mean surface temperatures, respectively.

Water-wall probe with both lateral and extended fins

$$Q_{t2} = m_w cp_w(T_{wo}-T_{wi})$$
$$= h_{avg}(A_{uf}+2A_{sf1}\times\eta_{f1}+A_{sf2}\times\eta_{f2})(T_B-T_S)$$

where A_{uf} is the surface area of the unfinned portion of the tube, A_{sf1} and A_{sf2} are the surface areas of lateral

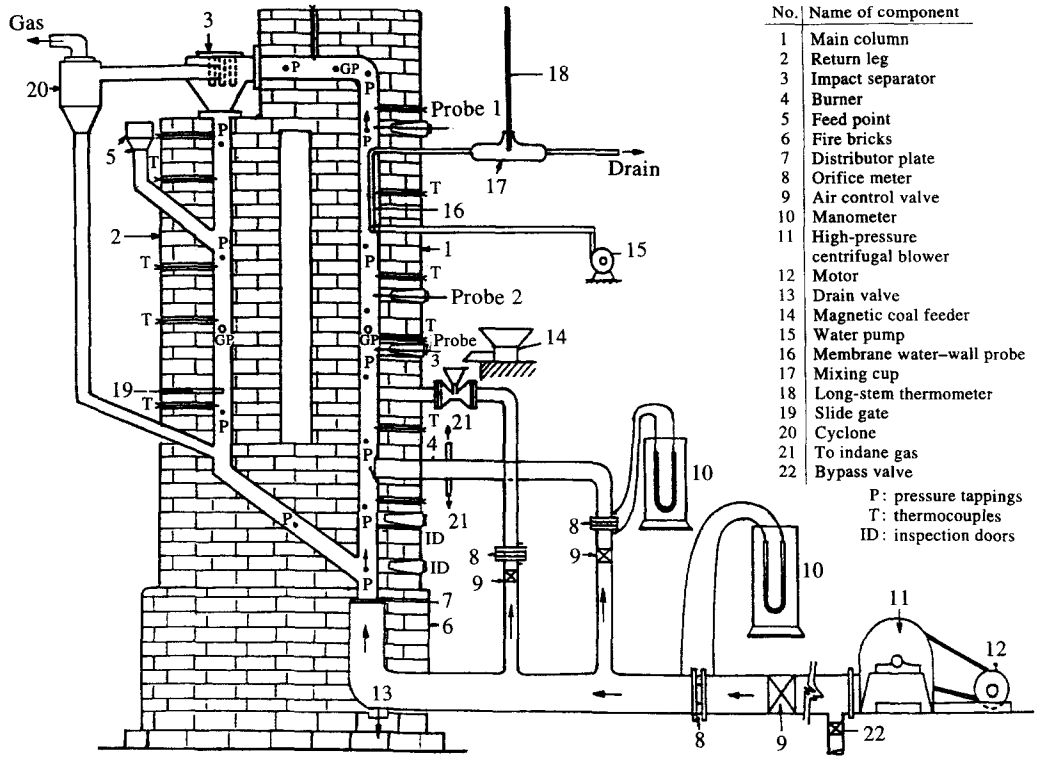

No.	Name of component
1	Main column
2	Return leg
3	Impact separator
4	Burner
5	Feed point
6	Fire bricks
7	Distributor plate
8	Orifice meter
9	Air control valve
10	Manometer
11	High-pressure centrifugal blower
12	Motor
13	Drain valve
14	Magnetic coal feeder
15	Water pump
16	Membrane water–wall probe
17	Mixing cup
18	Long-stem thermometer
19	Slide gate
20	Cyclone
21	To indane gas
22	Bypass valve

P: pressure tappings
T: thermocouples
ID: inspection doors

Fig. 1. Schematic diagram of experimental set-up.

and extended fins, respectively, η_{f1} and η_{f2} are the lateral and extended fin efficiencies, respectively. For lateral fins because of temperature symmetry the fin centre can be considered as of an insulated tip condition, ($dT/dx = 0$) and the fin efficiency is given by (only half of the lateral fin is considered on either side)

$$\eta_{f1} = \frac{\tanh m_1 b_1}{m_1 b_1}$$

where b_1 is the half of lateral fin length ($b_1 = 5$ mm).

For extended fin, the fin efficiency is given by

$$\eta_{f2} = \frac{\sinh m_2 b_2 + \dfrac{h_{avg}}{m_2 k_f}\cosh m_2 b_2}{\cosh m_2 b_2 + \dfrac{h_{avg}}{m_2 k_f}\sinh m_2 b_2} \times \frac{1}{m_2 b_{2c}}$$

where b_2 is extended fin length ($b_2 = 5$ mm). The corrected extended fin length b_{2c} is given by the approximation, $b_{2c} = b_2 + t/2$, where t is the thickness of the extended fin.

MODEL FORMULATION

A mathematical model has been proposed to predict the heat transfer rate from bed to the finned and unfinned surface of a water-wall in a CFB operating at a high temperature. The fin has been assumed to be of constant cross-section, having only one-dimensional heat conduction through it. The predominant mode of heat transfer from bed to the wall is of particle convection and radiation. The transport and thermal properties of the material have been assumed to be constant.

From energy balance (Fig. 3) the governing heat transfer equation for the control volume at steady-state can be written as

$$(q_c + q_r)P\,dx + A_f q_{x+dx} = q_x A_f \quad (1)$$

or

$$[h_{(x)}(T_B - T) + \sigma f_{wb}(T_B^4 - T^4)]P\,dx = -A_f \frac{d}{dx}\left(k_f \frac{dT}{dx}\right)dx \quad (2)$$

$$-k_f A_f \frac{d^2T}{dx^2} = h_{(x)}P(T_B - T) + \sigma f_{wb}P(T_B^4 - T^4) \quad (3)$$

where A_f is the cross-sectional area of the fin.

According to Glicksman [9] the convective heat transfer coefficient $h_{(x)}$ exhibits roughly the square root relationship with cross-sectional average suspension density, so that

$$h_{(x)} = C(\rho_{sus})^{1/2} = C(\rho_P(1-\varepsilon))^{1/2} \quad (4)$$

where C is a constant to be estimated by fitting the experimental data at room temperature conditions between $h_{(x)}$ and ρ_{sus}. Using the non-dimensional terms let $\xi = x/b$, where 'x' is the distance from the fin base and 'b' is the fin length.

Defining dimensionless temperatures for fin (θ) and bed (θ_b) as, $\theta = T/T_w$ and $\theta_b = T_B/T_w$ where T_B is the

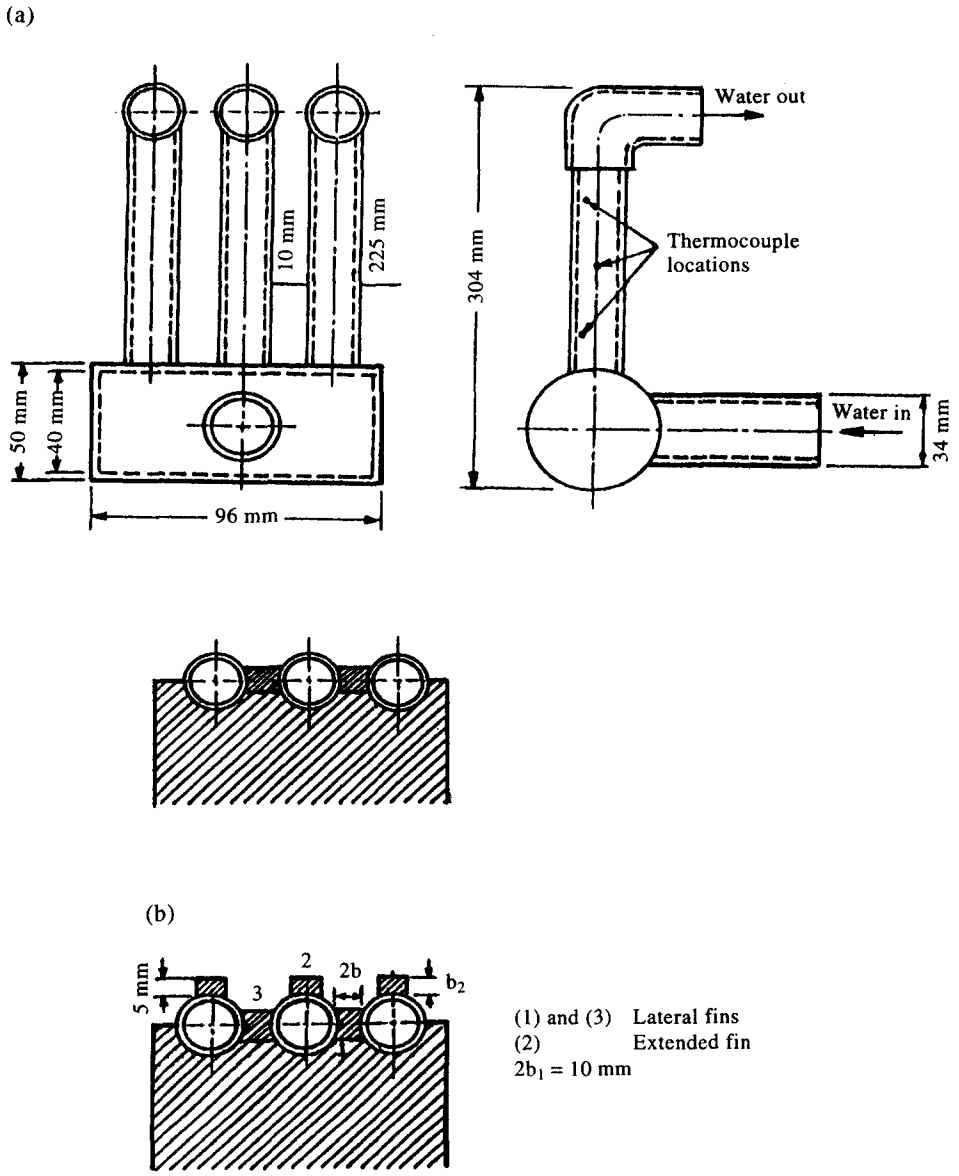

Fig. 2. (a) Schematic view of membrane water-wall heat transfer probe (lateral fins); (b) schematic view of finned water-wall heat transfer probe (lateral and extended fins).

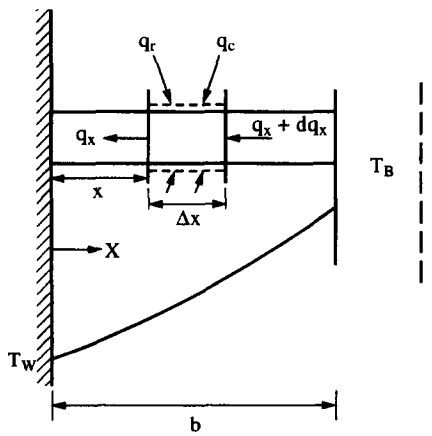

Fig. 3. Schematic view of the fin projecting from the water-wall tube.

bed temperature, T_w is the probe wall or fin base temperature and T is the surface temperature of fin at any location. The governing heat transfer equation (3) then becomes

$$T_w\, d^2\theta/d\xi^2 = -(Pb^2/A_f k_f)[(C\{\rho_p(1-\varepsilon)\}^{1/2})T_w(\theta_b-\theta) + \sigma f_{wb} T_w^4(\theta_b^4\theta^4)]. \quad (5)$$

Dividing by T_w

$$d^2\theta/d\xi^2 = -(Pb^2/A_f k_f)[(C\{\rho_p(1-\varepsilon)\}^{1/2})(\theta_b-\theta) + \sigma f_{wb} T_w^3(\theta_b^4-\theta^4)]$$

or

$$d^2\theta/d\xi^2 = -(Pb^2/A_f k_f)[h_{(x)}+h_{rad}](\theta-\theta_b). \quad (6)$$

The radiation heat transfer coefficient h_{rad} is modeled as given by Basu [10] as

$$h_{rad} = \delta h_{rc} + (1-\delta) h_{rd}$$

$$h_{rad} = [\delta f_{wc} + (1-\delta) f_{wd}] \sigma (T_B^4 - T_4)/(T_B - T) \quad (7)$$

$$h_{rad} = [\delta f_{wc} + (1-\delta) f_{wd}] \sigma T_w^3 (\theta_b^2 + \theta^2)(\theta_b + \theta) \quad (8)$$

where δ is the fraction of the wall area covered by clusters and $(1-\delta)$ is the area covered by dispersed phase and h_{rc} and h_{rd} are the radiative components for the cluster and dispersed phase, respectively.

The fraction of the wall area covered by clusters, δ, may be written approximately from the expression used by Basu and Nag [11], which has been modified by Nag and Ali [12] as (with short fins, no equation exists for δ, so approximately this is taken)

$$\delta = (1-\varepsilon_w - y)/(1-\varepsilon_c - y) \quad (9)$$

where $y = 0.001$, $\varepsilon_c = 0.5$, and ε_w voidage at the wall.

The wall-to-cluster and wall-to-dispersed phase view factors are given as

$$f_{wc} = \frac{1}{(1/e_w + 1/e_c - 1)} \quad (10)$$

$$f_{wd} = \frac{1}{(1/e_w + 1/e_d - 1)} \quad (11)$$

where e_w is the emissivity of the wall, and e_c is the emissivity of the cluster which is given as (Grace [13])

$$e_c = 0.5(1 + e_p)$$

where e_p is the emissivity of the particle and e_d is the emissivity of the dispersed phase. According to Basu and Nag [14], the emissivities for cluster and dispersed phase range between 0.85 and 0.95, so e_d of 0.95 is chosen for the dispersed phase. Thus, equation (6) can be written as

$$d^2\theta/d\xi^2 - m^2(\theta - \theta_b) = 0$$

$$\text{where } m^2 = hPb^2/A_f k_f. \quad (12)$$

Boundary conditions

Lateral fin. For fins 1 and 3 (lateral fins) [Fig. 2(b)]

$$\theta_{x=0^{(0)}} = \theta_{\xi=0} = T(0)/T_w = 1$$

at $x = b$, $\xi = 1$, $d\theta/d\xi|_{\xi=1} = 0$ (because of temperature symmetry the dT/dx is assumed to be zero at the centre of the fin). The dimensionless temperature distribution for fins 1 and 3 (lateral fins) is given as

$$\frac{\theta - \theta_b}{\theta_1 - \theta_b} = \frac{\cosh m_1(1-\xi)}{\cosh m_1}. \quad (13)$$

For the extended fin:

$$\theta_{x=0^{(0)}} = \theta_{\xi=0} = T(0)/T_w = 1$$

$$k_f\, dT/dx|_{x=b} = h(T_B - T)$$

$$\text{or} \quad k_f\, d\theta/b\, d\xi|_{\xi=1} = h(\theta b - \theta).$$

The dimensionless temperature distribution for fin 2 (extended fin) is given by

$$\frac{\theta - \theta_b}{1 - \theta_b} = \left[\frac{\cosh m_2(1-\xi) + \dfrac{hb_2}{m_2 k_f} \sinh m_2(1-\xi)}{\cosh m_2 + \dfrac{hb_2}{m_2 k_f} \sinh m_2} \right]. \quad (14)$$

The heat transfer rate through the lateral fin (fins 1 and 3) at steady-state is given by

$$Q_{f1} = k_f A_{f1} (T_w/b)\, d\theta/d\xi|_{\xi=0} \quad (15)$$

The heat transfer rate through the extended fin (Fin 2) at steady-state is given by

$$Q_{f2} = k_f A_{f2} (T_w/b)\, d\theta/d\xi|_{\xi=0} \quad (16)$$

and for the unfinned portion of the water-wall tube surface

$$Q_{uf} = h A_{uf} T_w (\theta_b - \theta). \quad (17)$$

Total heat transfer through the water-wall probe with both lateral and extended fins is given by

$$Q_{tot} = Q_{uf} + 2Q_{f1} + Q_{f2}. \quad (18)$$

The equivalent heat transfer coefficient based on the total surface area for the test section with lateral and extended fins is given by

$$h_{eq} = \frac{Q_{tot}}{A_{tot} T_w (\theta_b - \theta)} \quad (19)$$

The fin efficiencies for various extended fin lengths are estimated by calculating the maximum possible heat transfer rate through the fin at ideal conditions. The constant C in equation (4) is evaluated by fitting the experimental results between $h_{(x)}$ and ρ_{sus}, for the probe with lateral and extended fins at room temperature conditions.

RESULTS AND DISCUSSION

the variation of heat transfer coefficient with suspension density for the probe is plotted in Fig. 4. The heat transfer coefficient increases with suspension density in consistence with earlier works [3–5, 9, 11].

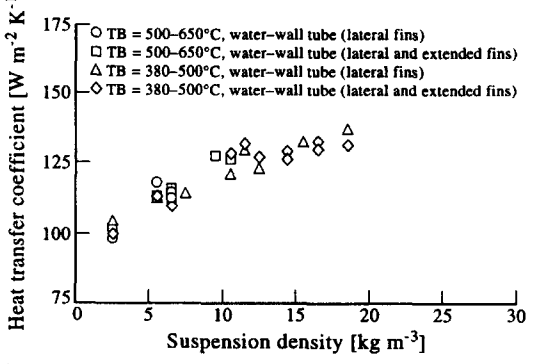

Fig. 4. Heat transfer coefficient vs suspension density for water-wall tube with lateral fins, and water-wall tube with lateral as well as extended fins.

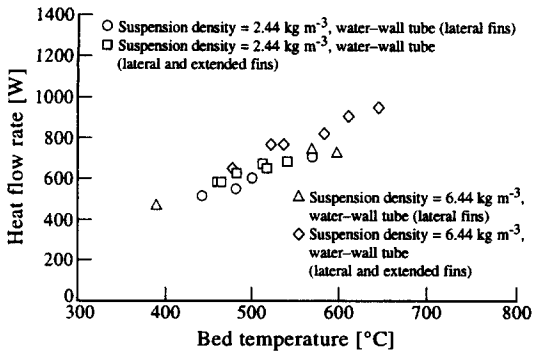

Fig. 5. Comparison of heat flow rate with bed temperature for water-wall probe, SG = 10 cm^2.

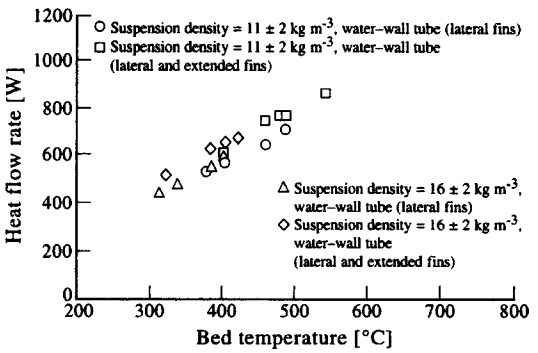

Fig. 6. Effect of bed temperature on heat flow rate for the water-wall probe with different suspension density ranges, SG = 10 cm^2.

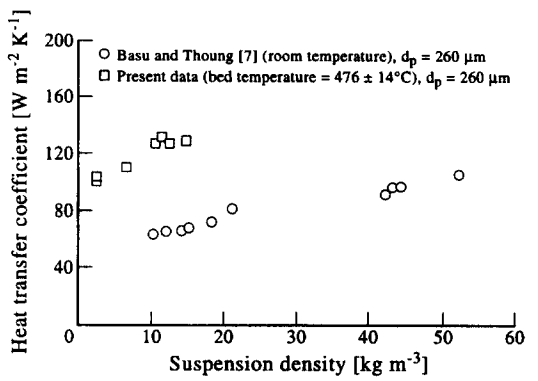

Fig. 7. Comparison of present experimental data of water-wall heat transfer probe with both lateral and extended fins with Basu and Thoung (1993).

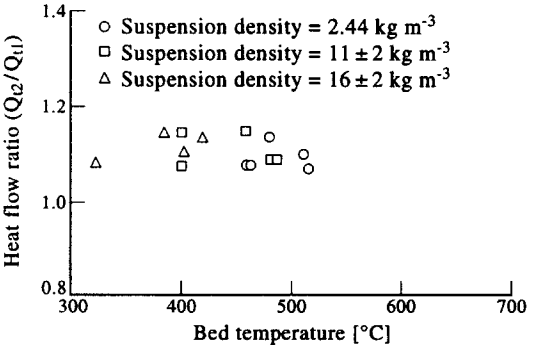

Fig. 8. Heat flow ratio variation for the water-wall probe with bed temperature.

The results also demonstrate that the addition of an extended fin to the water-wall probe with lateral fins, results in a little drop in the heat transfer coefficient. The heat flow rate variation with bed temperature is shown in Figs. 5 and 6. The addition of the extended fin increases the heat absorption from the bed compared to lateral fin, thereby increasing the heat flow rate. For lateral fins only one side of the fin surface is effective for heat absorption, and in the case of the extended fin, whole surface is effective for heat absorption.

The comparison of present experimental data with that of Basu and Ngo [7] is shown in Fig. 7. The trends are the same and the deviations are attributed to the probe size and operating conditions. The heat flow ratio (Q_{t2}/Q_{t1}) variation with bed temperature is demonstrated in Fig. 8. Due to the addition of extended fin, the heat transfer surface area increases by 15.3%, but the corresponding increase in heat flow rate is between 7 and 14% (heat flow ratio varies between 1.07 and 1.14).

The model results are obtained for different bed temperature ranges. Sand with a mean size (d_p) 248 μm and particle density of 2350 kg m^{-3} is considered for model calculations. The variation of equivalent probe heat transfer coefficient with suspension density is presented in Fig. 9 for two bed temperature ranges. This includes the radiation part also. As can be observed, the heat transfer coefficient increases with the suspension density. For the same suspension density range, the heat transfer coefficient increases with the bed temperature. The increase in suspension density causes more particles near the wall, which results in more heat transfer to the surface, thereby increasing the heat transfer coefficient.

The present model results are plotted with suspension density along with published literature in Fig.

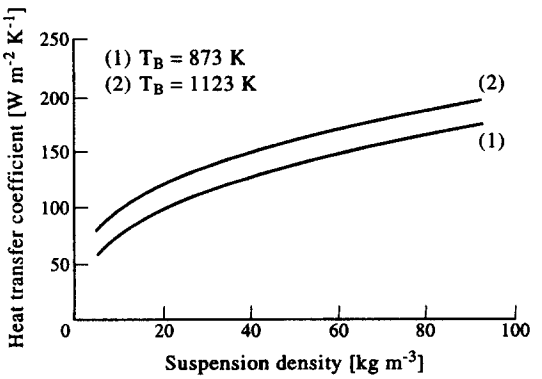

Fig. 9. Effect of suspension density on heat transfer coefficient, analytical model results.

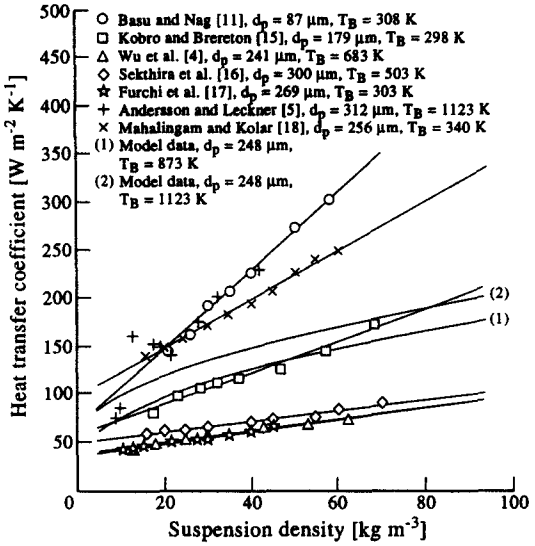

Fig. 10. Heat transfer coefficient variation with suspension density, comparison of model results with the published literature.

10. The model also predicts the variation of heat transfer coefficient with suspension density along the same lines as reported in the literature. The comparison is made only to see the nature of heat transfer coefficient with suspension density. The deviations of the model results with literature can be attributed to different probe sizes and temperatures as used by different investigators.

Figure 11 shows the comparison of experimental and model heat flow rates for the water-wall probe of the same dimensions (15 mm ID, 22.5 mm OD and 304 mm in height with lateral and extended fins of 190 mm (height) × 5 mm (length) × 5 mm (thickness)). The model heat flow rates are in fairly good agreement with the experimental data. The deviation can be attributed to the assumptions made in the model formulation and also to the properties and constants that are used in the model.

The fin efficiencies for various extended fin lengths

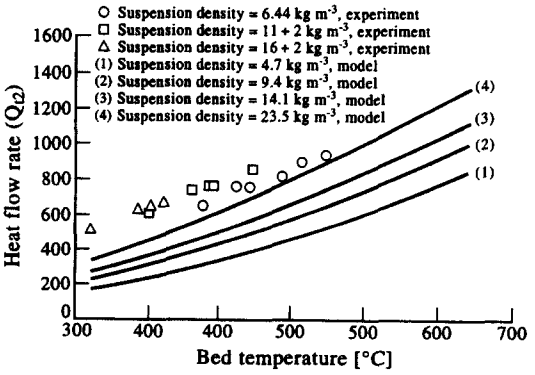

Fig. 11. Comparison of experimental and model heat flow rates at different bed temperatures for the probe with both lateral and extended fins.

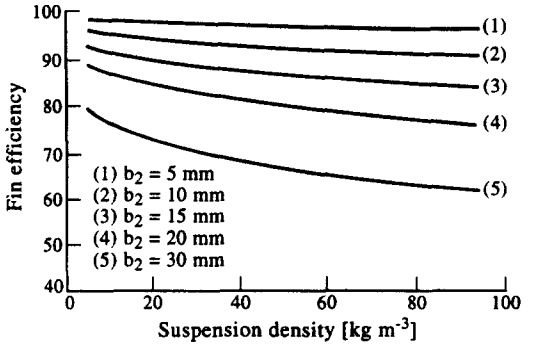

Fig. 12. Extended fin efficiency vs suspension density for various fin widths (b_2), T_θ = 1123 K.

are shown in Fig. 12. The fin efficiency decreases with an increase in fin length. The increase in fin length may affect bed hydrodynamics, which in turn affects the heat transfer rate. So far with longer fins, the efficiency decreases with suspension density.

The heat flux (Q_{tot}/A_{tot}) variation for various extended fin lengths are presented in Fig. 13, for various suspension density ranges. Up to a certain extended fin length the heat flux remains more or less the same and afterwards it starts decreasing at a faster rate indicating that the short extended fins may be more effective in absorbing heat from the bed. The short fins may not affect much of bed hydrodynamics, whereas the long fins will result in different bed hydrodynamics, which in turn result in reduced heat transfer to the fins. So small extended fins may be preferred because they increase heat absorption, as observed in the present investigation.

CONCLUSION

The heat flow rate increases with bed temperature and suspension density. The addition of a short extended fin, to the probe with lateral fins, increases the heat absorption from the bed. The heat flow ratio does not increase in the same proportion as that of area ratio. The model results are compared with the experimental data and also with the published literature and the results are in fairly good agreement. It

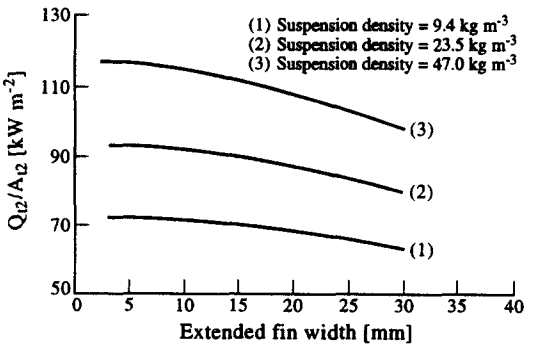

Fig. 13. Q_{t2}/A_{t2} for water-wall probe with both lateral and extended fins with extended fin width (b_2) model results, TB = 1123.16 K.

seems that short extended fins may be more effective in increasing the heat flow rate from the bed to the water-wall tubes. For the extended fin, the fin efficiency decreases with an increase in fin length.

REFERENCES

1. Basu, P., Ali Moral, M. N. and Nag, P. K., An experimental investigation into the effect of fins on heat transfer in circulating fluidized beds. *International Journal of Heat and Mass Transfer*, 1991, **34,** 2317–2326.
2. Nag, P. K. and Ali Moral, M. N., An experimental study of the effect of pin-fins on heat transfer in circulating fluidized beds. *International Journal of Energy Research*, 1993, **17,** 863–872.
3. Wu, R. L., Lim, C. J., Chaouki, Jamal and Grace, J. R., Heat transfer from a circulating fluidized bed to membrane water-wall surfaces. *A.I.Ch.E.J.*, 1987, **35,** 1881–1892.
4. Wu, R. L., Grace, J. R., Lim, C. J. and Brereton, C. M. M., Suspension-to-surface heat transfer in circulating fluidized bed combustor. *A.I.Ch.E.J.*, 1989, **35,** 1685–1691.
5. Andersson, B. A. and Leckner, B., Experimental methods of estimating heat transfer in circulating fluidized bed boilers. *International Journal of Heat and Mass Transfer*, 1992, **35,** 3353–3362.
6. Golriz, M. R., Investigation of heat transfer characteristics in a 12 MW circulating fluidized bed boiler. In *Heat and Mass Transfer* 94, eds A. R. Balakrishnan and S. S. Murthy. McGraw-Hill, New Delhi, 1994, pp. 973–978.
7. Basu, P. and Ngo, T., Effect of some operating parameters on heat transfer to vertical fins in a circulating fluidized bed furnace. *Powder Technology*, 1993, **74,** 249–258.
8. Reddy, B. V. and Nag, P. K., Fin heat transfer studies in a high temperature circulating fluidized beds. In *VIII International Congress and Exhibition*, New Delhi, eds P. K. Gupta and B.S.K. Naidu. 1994, pp. 71–78.
9. Glicksmann, L. R., Circulating fluidized bed heat transfer. In *Circulating Fluidized Bed Technology II*, P. Basu and J. F. Large. Pergamon Press, Oxford, 1988, pp. 13–29.
10. Basu, P., Heat transfer in high temperature fast beds. *Chemical Engineering Science*, 1990, **45,** 3123–3136.
11. Basu, P. and Nag, P. K., An investigation into heat transfer in circulating fluidized beds. *International Journal of Heat and Mass Transfer*, 1987, **30,** 2399–2409.
12. Nag, P. K. and Sallam Ali, M., Effect of operating parameters on bed-to-wall heat transfer in a high temperature circulating fluidized bed. *International Journal of Energy Research*, 1992, **16,** 61–73.
13. Grace, J. R., Heat transfer in circulating fluidized beds. In *Circulating Fluidized Bed Technology I*, ed. P. Basu. Pergamon Press, Canada, 1986, pp. 63–81.
14. Basu, P. and Nag, P. K., A review on heat transfer to walls of a circulating fluidized bed furnace. *Chemical Engineering Science*, 1996, **26,** 1–26.
15. Kobro, H. and Brereton, C., Control and fuel flexibility in circulating fluidized beds. In *Circulating Fluidized Bed Technology I*, ed. P. Basu. Pergamon Press. Canada, 1986, pp. 263–272.
16. Sekthira, A., Leey, Y. and Genetti, W. E., Heat transfer in a circulating fluidized bed. *25th International Heat Transfer Conference*, Houston, TX, 1988, pp. 24–27.
17. Furchi, J. C. L., Goldstein Jr, L., Lombardi, G. and Mohseni, M., Experimental local heat transfer in a circulating fluidized bed. In *Circulating Fluidized Bed Technology II*, eds P. Basu and J. F. Large. Pergamon Press, Oxford, 1988, pp. 263–270.
18. Mahalingam, M. and Kolar, A. K., Experimental correlation for average heat transfer coefficient at the wall of a circulating fluidized bed. *4th International Conference on CFB*, Pittsburgh, PA, 1993, pp. 390–395.